



Published in final edited form as:

J Neurosurg. 2013 February ; 118(2): 465–477. doi:10.3171/2012.10.JNS111836.

Evaluation of the hematoma consequences, neurobehavioral profiles, and histopathology in a rat model of pontine hemorrhage:

Laboratory investigation

Tim Lekic, M.D., Ph.D.¹, William Rolland, B.S.¹, Anatol Manaenko, Ph.D.¹, Paul R. Krafft, M.D.¹, Joel E. Kamper, M.A.⁴, Hidenori Suzuki, M.D., Ph.D.¹, Richard E. Hartman, Ph.D.⁴, Jiping Tang, M.D.¹, and John H. Zhang, M.D., Ph.D.^{1,2,3}

¹Department of Physiology and Pharmacology, School of Medicine, Loma Linda University, Loma Linda, California

²Department of Anesthesiology, School of Medicine, Loma Linda University, Loma Linda, California

³Department of Neurosurgery, School of Medicine, Loma Linda University, Loma Linda, California

⁴Department of Psychology, School of Science and Technology, Loma Linda University, Loma Linda, California

Abstract

Object—Primary pontine hemorrhage (PPH) represents approximately 7% of all intracerebral hemorrhages (ICHs) and is a clinical condition of which little is known. The aim of this study was to characterize the early brain injury, neurobehavioral outcome, and long-term histopathology in a novel preclinical rat model of PPH.

Methods—The authors stereotactically infused collagenase (Type VII) into the ventral pontine tegmentum of the rats, in accordance with the most commonly affected clinical region. Measures of cerebrovascular permeability (brain water content, hemoglobin assay, Evans blue, collagen Type IV, ZO-1, and MMP-2 and MMP-9) and neurological deficit were quantified at 24 hours postinfusion (Experiment 1). Functional outcome was measured over a 30-day period using a vertebrobasilar scale (the modified Voetsch score), open field, wire suspension, beam balance, and inclined-plane tests (Experiment 2). Neurocognitive ability was determined at Week 3 using the rotarod (motor learning), T-maze (working memory), and water maze (spatial learning and memory) (Experiment 3), followed by histopathological analysis 1 week later (Experiment 4).

Results—Stereotactic collagenase infusion caused dose-dependent elevations in hematoma volume, brain edema, neurological deficit, and blood-brain barrier rupture, while physiological variables remained stable. Functional outcomes mostly normalized by Week 3, whereas

Address correspondence to: John H. Zhang, M.D., Ph.D., Department of Physiology and Pharmacology, Loma Linda University School of Medicine, 11041 Campus Street, Risley Hall, Room 219, Loma Linda, California 92354. johnzhang3910@yahoo.com..

Disclosure

The authors report no conflict of interest concerning the materials or methods used in this study or the findings specified in this paper.

Author contributions to the study and manuscript preparation include the following. Conception and design: Zhang. Acquisition of data: Lekic, Rolland, Manaenko, Tang. Analysis and interpretation of data: Lekic, Krafft. Drafting the article: Lekic, Krafft. Critically revising the article: all authors. Reviewed submitted version of manuscript: all authors. Approved the final version of the manuscript on behalf of all authors: Zhang. Statistical analysis: Hartman. Administrative/technical/material support: Manaenko, Kamper, Suzuki, Tang. Study supervision: Zhang, Hartman.

neurocognitive deficits paralleled the cystic cavitory lesion at 30 days. Obstructive hydrocephalus did not develop despite a clinically relevant 30-day mortality rate (approximately 54%).

Conclusions—These results suggest that the model can mimic several translational aspects of pontine hemorrhage in humans and can be used in the evaluation of potential preclinical therapeutic interventions.

Keywords

pontine hemorrhage; neurobehavioral testing; histopathology; rat; vascular disorders

Primary pontine hemorrhage is a subtype of ICH resulting from the spontaneous rupture of perforating (paramedian) basilar artery branches into the ventral pontine tegmental junction with the basis pontis.^{52,117,138} This devastating injury has a yearly incidence of 1 per 50,000 people, accounting for approximately 140,000 (approximately 7%) of 2 million worldwide ICHs^{32,102} and having a 65% mortality rate despite contemporary medical-surgical approaches.^{31,80,137}

Uncontrolled hematoma expansion worsens patient outcomes after pontine hemorrhage.^{3,8,26,39,85,128} In addition, approximately half of the survivors will acquire lesions that cause lasting cognitive deficits in motor learning and visuospatial ability.^{74,75,88} Greater disability occurs after larger and bilaterally extending hematomas.^{10,15,60,98} This deterioration, however, is poorly understood¹⁰² and is a clinical burden that underscores the need for further translational work.^{56,87}

Collagenase-induced ICH in rodents is a useful tool for therapeutic investigations of hemostasis, neurobehavior, and histopathology outcomes.^{1,33,71,105,121} Our preliminary report showed the feasibility of pontine hemorrhage in this animal model, using an established pontine infusion approach^{66,91} modified by the collagenase ICH modeling technique.¹⁰⁵ This is shown to avoid the limitation of intraventricular bleeding found after experimental autologous blood infusion into the brainstem.¹⁶ In the present study, therefore, we hypothesized that this rodent model of collagenase infusion can mimic outcomes after spontaneous pontine hemorrhage in humans, for use in the further evaluation of therapeutic interventions.^{3,10,26,39,60,75,98,114,128}

Methods

Animals and Operative Procedure

In this present study we used 109 adult male Sprague-Dawley rats (Harlan) weighing 290-345 g. All procedures were in full compliance with the *Guide for the Care and Use of Laboratory Animals* (NIH publication no. 85-23) and were approved by the Institutional Animal Care and Use Committee at Loma Linda University. Surgeries involved isoflurane anesthesia (4% induction, 2% maintenance, 70% medical air, and 30% O₂), and all procedures included standard aseptic techniques. The anesthetized animals were secured prone onto a stereotactic frame (Kopf Instruments) and an incision was then made over the scalp. The following stereotactic coordinates were measured over the exposed cranium (caudally, laterally, and to a depth) from the bregma to localize the right ventral pontine tegmentum: 10.2 mm (caudal), 1.4 mm (lateral), and 9.15 mm (deep). Using a standard dental drill, a 1-mm borehole was then formed, through which a 27-gauge needle was inserted, and collagenase Type VII-S (0.2 U/ μ l; Sigma) was infused by microinfusion pump (Harvard Apparatus) at a rate of 0.2 μ l/minute. The syringe remained in place for 10 minutes to prevent back-leakage before being slowly withdrawn (1 mm/minute). A thermostat-controlled heating blanket maintained the core temperature (37.0°C \pm 0.5°C)

throughout the entire operation. Control surgeries consisted of needle insertion alone. The borehole was then sealed with bone wax, the incision was sutured closed, and the animals were followed during the recovery period. Food, water, and postoperative supportive care were provided, as is routinely done.⁴² Dose-dependent infusions (0.15 and 0.3 U collagenase) were used in the short-term 24-hour study (that is, Experiment 1 [hemorrhagic volume, brain water content, neuroscore, physiological variables {Table 1}, and vascular permeability, Western blot]). Thereafter, infusions of 0.15 U collagenase were evaluated in the long-term 30-day outcome studies (that is, Experiments 2-4 [neurological function, neurological cognition, and histopathology]).

Hematoma Consequences at 24 Hours (Experiment 1)

Animal Perfusion and Tissue Extraction—The animals were fatally anesthetized with isoflurane (5%) followed by cardiovascular perfusion with ice-cold PBS for the hemoglobin and Evans blue assays, and immunoblot analyses. The brainstem was then dissected and snapfrozen with liquid nitrogen, and then stored at -80°C , before spectrophotometric quantification or protein extraction. Because the hematoma was stereotactically induced, but edema is known to spread, the hemorrhage volume was quantified using only the extracted brainstem tissue, whereas brain water content was also measured in adjacent structures (that is, cerebral and cerebellar hemispheres).

Hemorrhagic Volume—The spectrophotometric hemoglobin assay was performed using well-established protocols.^{14,119} Extracted brainstem tissue was placed in glass test tubes with 3 ml of PBS and then homogenized for 60 seconds (Tissue Miser Homogenizer, Fisher Scientific). Ultrasonication for 1 minute lysed erythrocyte membranes, the products were centrifuged for 30 minutes, and Drabkin reagent was added (Sigma-Aldrich) into aliquots of supernatant fluid that reacted for 15 minutes. Absorbance, using a spectrophotometer (540 nm; Genesis 10uv, Thermo Fisher Scientific), was calculated into a hemorrhagic volume on the basis of a standard curve.

Brain Water Content—The percentage of brain edema was measured using the wet-weight/dry-weight method.¹¹⁹ Quickly after sacrifice, the brains were removed and divided. The tissue weights were determined before and after drying for 24 hours in a 100°C oven by using an analytical microbalance (model AE 100, Mettler Instrument Co.) capable of measuring with a $1.0\text{-}\mu\text{g}$ precision. The data were calculated as the percentage of water content: $(\text{wet weight} - \text{dry weight})/\text{wet weight} \times 100$.

Neuroscore—Composite neurological evaluation is a sensorimotor value consisting of the combined averages from wire suspension, beam balance, and inclined plane.^{19,30} The Voetsch neuroscore (Table 2) is a modified vertebrobasilar scale score of sensorimotor ability.^{47,123} The neuroscore was calculated as percentage difference (subtraction) of the mean performance from shams. Values are expressed as percentage of sham (further details provided in Experiment 2).

Physiological Variables and Vascular Permeability Measurement—Under general anesthesia (operatively), the right femoral artery was catheterized and physiological parameters were measured, reassessed 24 hours later on the opposite (left) side; this was followed by intravenous injection of 2% Evans blue (5 ml/kg, 1-hour circulation), as is routinely done.⁶⁴ Extracted brainstem tissue was then weighed, homogenized in 1 ml PBS, and finally centrifuged for 30 minutes. The supernatant fluid (0.6 ml) was added with equal volumes of trichloroacetic acid, and this was followed by a temporal pause and (biochemical) overnight incubation and recentrifugation the next day. The final supernatant

fluid underwent spectrophotometric quantification (615 nm; Genesis 10uv, Thermo Fisher Scientific) of extravasated dye, as previously described.¹⁰⁹

Western Blot Analysis—For protein immunoblot,¹¹⁹ the concentration of protein was determined using the DC Protein Assay (Bio-Rad). Samples were subjected to SDS-PAGE (sodium dodecyl sulfate polyacrylamide gel electrophoresis) and then transferred to nitrocellulose membrane for 80 minutes at 70 V (Bio-Rad). Blotting membranes were incubated for 2 hours with 5% nonfat milk in Tris-buffered saline containing 0.1% Tween 20 and were then incubated overnight with the following primary antibodies: anticollagen IV (1:500; Chemicon), anti-ZO-1 (1:500; Invitrogen Corp.), anti-MMP-2 and anti-MMP-9 (1:1500; Millipore), followed by incubation with secondary antibodies (1:2000; Santa Cruz Biotechnology) and processing with the ECL Plus kit (Amersham Bioscience). Images were semiquantitatively analyzed using ImageJ (4.0, Media Cybernetics).

Neurofunctional Profiles at 30 Days (Experiment 2)

Animals were assessed using a battery of functional outcome measures. For the Voetsch neuroscore (maximum score 42), the sum of 14 parameters of a vertebrobasilar scale⁴⁷ was recorded (Table 2); scores for each parameter ranged from 3 (no neurological deficit) to 0 (complete neurological deficit). For locomotion, the path length in open-topped plastic boxes (49 cm long × 35.5 cm wide × 44.5 cm tall) was digitally recorded for 30 minutes and analyzed by Noldus EthoVision tracking software.^{42,64} For sensorimotor function, the falling latency was recorded (60 second cut-off) when all four limbs were placed perpendicularly onto a stationary horizontal beam balance (50 cm in length × 5 cm in diameter) or as the forelimbs grasped onto the wire suspension (40 cm in length × 3 mm in diameter).¹⁹ The inclined plane consisted of a box (70 cm long × 20 cm wide × 10 cm tall) with an analog protractor and hinged base, elevated at 5° intervals until the animal slipped backward.³⁰

Neurocognitive Ability at the 3rd Week (Experiment 3)

Higher-order brain function was measured using a panel of specific tests. For the rotarod task, a motor-learning paradigm was assessed by comparing preoperative performance with four daily blocks on the 3rd week after injury on Days 21, 23, 25, and 27.^{42,62} The apparatus consisted of a horizontal rotating cylinder (7 cm in diameter × 9.5 cm in width, acceleration 2 rpm/5 sec) requiring continuous walking to avoid falling, which was recorded by photobeam-circuit (Columbus Instruments). The T-maze assessed short-term (working) memory.⁵⁰ Rats were placed into the stem (40 × 10 cm) of a maze and allowed to explore until one arm (46 × 10 cm) was chosen. From the sequence of 10 trials, of left and right arm choices, the rate of spontaneous alternation was calculated (range 0% [no alteration/trial] to 100% [complete, alternations/trial]).^{28,136} For the Morris water maze task, spatial learning and memory were assessed over 4 daily blocks on Days 22, 24, 26, and 28.^{42,62} The apparatus consisted of a metal pool (diameter 110 cm), filled to within 15 cm of the upper edge, with a platform (diameter 11 cm) for the animal to escape onto that changed location for each block (maximum 60 sec/trial); trials were digitally analyzed using Noldus EthoVision tracking software. Cued trials measured place learning with the escape platform visible above water; spatial trials measured spatial learning with the platform submerged; and probe trials measured spatial memory once the platform was removed.

Histopathology at 30 Days (Experiment 4)

The animals were terminally anesthetized with isoflurane (5%) and transcardially perfused with ice-cold PBS and then 10% paraformaldehyde. The brains were removed and postfixed in 10% paraformaldehyde, followed by 30% sucrose (weight/volume) for 3 days. All

histopathological analyses used 10- μ m-thick coronal sections caudally cut every 800 μ m on a cryostat (LM3050S, Leica Microsystems) that were mounted and stained on poly-L-lysine-coated slides. Morphometric analysis of cresyl violet slides⁶⁴ involved computer-assisted (ImageJ 4.0) hand delineation of the ventricle system (lateral, third, cerebral aqueduct, and fourth), cerebellum (ipsi- and contralateral), brainstem (midbrain, pontine, and medulla), and lesioned area (cavity, cellular debris). Borderlines were based on criteria defined from stereological studies that used optical dissector principles.^{2,5,27,94,103,120} Brain tissue volumes were calculated over 8 sequential sections (every 800 μ m; 7.4-13 mm from the bregma) using established methods: [(average [(area of coronal section) – (lesion area)] \times interval \times number of sections)].⁷¹ To account for variant neuronal densities in the brainstem (midbrain, pontine, and medulla), the relative loss of cell density was estimated using established protocols,^{71,99,111,113} where the cells were counted using \times 400 magnification over 5 equidistant areas (250 \times 250- μ m grids) per brainstem side (ipsi- and contralateral).^{29,64} The relative loss of neurons was then determined by subtracting the difference in averages of the two sides,⁶² and the final value was expressed as the neuronal losses per brainstem region. All measurements were performed blinded and twice repeated.

Statistical Analysis

Statistical significance was considered at an α -level of $p < 0.05$. Data were analyzed using ANOVA, and with repeated-measures ANOVA for the long-term neurobehavior analysis. Significant interactions were then further explored with the conservative Scheffe post hoc test, t-test (unpaired), and Mann-Whitney rank sum test, when appropriate.

Results

Experimental Model of Pontine Hemorrhage in the Rat

Systemic physiological parameters were stable during and after (1 and 30 days) the surgical procedure (Table 1). Under isoflurane anesthesia, the nonparalyzed animals breathed spontaneously (no ventilator), and blood gases were monitored intra- and postoperatively, as is routinely done during experimental rat collagenase brain infusion studies.^{42,64} Within 30 minutes of waking from anesthesia, the collagenase pontine-infused animals, as determined by our qualitative observations, exhibited ataxic gaits, craniocaudal rotations, and cranial nerve and limb dysfunctions. These neurological deficits, similar to those previously described following posterior brain circulation injury in rats,⁴⁷ formed the basis of our qualitative neuroscore, as defined in Table 2. Repeated gross pathological examination (during tissue preparation for biochemical or morphological analyses) revealed well-localized hematomas within the right ventral tegmental pons, without subarachnoid (or subdural) bleeding and without any ventricular obstruction (Fig. 1B and C). The timing of animal deaths in this study is demonstrated using the Gehan-Breslow survival graphs (Fig. 1D and E). The mortality rates were 8% and 25% at 24 hours (0.15 and 0.3 U, respectively [Fig. 1D]; Experiment 1), and 54% over 30 days (0.15 U [Fig. 1E]; Experiments 2-4). Non-survivor data were excluded from study.

Hematoma Consequences at 24 Hours (Experiment 1)

Unilateral collagenase infusion led to dose-dependent elevations of hematoma volume, brain water content, neurological deficits, and vascular permeability ($p < 0.05$; Fig. 2A-D). Immunoblots showed significant elevation of MMP-2 and -9 and degradation of collagen Type IV and ZO-1 ($p < 0.05$; Fig. 2E).

Neurofunctional Profiles Over 30 Days (Experiment 2)

Infusion of collagenase (0.15 U) led to significant neurological (modified Voetsch score), locomotor (open field), and sensorimotor (wire suspension, beam balance, and inclined plane) deficits over the 1st week postinjury ($p < 0.05$; Fig. 3A-F), in spite of stable body weights ($p > 0.05$). Most functional parameters recovered before the 3rd week ($p > 0.05$) after collagenase infusion, except for that measured for the inclined plane, which continued to show differences compared with the controls ($p < 0.05$; Fig. 3F).

Neurocognitive Ability at Week 3 (Experiment 3)

Collagenase (0.15 U)-infused animals performed significantly worse than controls over all postoperative rotarod (motor) testing blocks ($p < 0.05$; Fig. 4A) and were unable to improve upon their preoperative performance ($p > 0.05$), whereas the controls progressively improved their falling-latency time ($p < 0.05$). Although T-Maze results showed a significant loss of “working” memory ($p < 0.05$; Fig. 4B), the water-maze demonstrated equal “place learning” (cued trials) for all groups ($p > 0.05$; Fig. 4C). On the spatial blocks, however, collagenase-infused animals performed significantly worse than controls ($p < 0.05$) and were unable to improve upon their place-learning performance ($p > 0.05$). In comparison, controls performed progressively better with each block ($p < 0.05$; Fig. 4C) and with the spatial memory probe ($p < 0.05$; Fig. 4D).

Histopathology at 30 Days (Experiment 4)

The topography of the right tegmental pontine lesion extended within the brainstem in a Gaussian distribution, surrounding the level of injection (10.2 mm caudal from the bregma; Fig. 5A). The cystic cavitory lesion caused focal atrophic losses of brainstem tissue volume ($p < 0.05$; Fig. 5B, C, and E), without affecting the size of the cerebellar hemispheres ($p > 0.05$; Fig. 5C). The ventricles remained patent and unchanged in size ($p > 0.05$; Fig. 5D). Quantifiably, the greatest percentage of atrophy was pontine ($36.9\% \pm 6.2\%$, $p < 0.05$; Fig. 5E), in comparison with the midbrain ($16\% \pm 5.3\%$) and medulla ($14\% \pm 5.7\%$). However, the neuronal densities were diffusely diminished (pontine 8.63 ± 2.7 ; midbrain 5.35 ± 2.8 , medulla 5 ± 2.2 ; Fig. 5F).

Discussion

A requisite priority of translational stroke research is the characterization of appropriate experimental ICH models.⁸⁷ Animal models of posterior circulation hemorrhage help demonstrate the unique features of cerebellar⁶⁴ and pontine⁶⁶ lesions in comparison with other brain injury sites.⁶⁷ This is particularly important because clinical studies do not adequately address this patient population.^{72,73} The use of autologous blood or collagenase infusion into the basal ganglia region of rodents represents the currently most common experimental approaches for studying this condition.^{1,71,129} However, basal ganglia hemorrhage is a deep cerebral bleeding subtype that, as a group (basal ganglia, thalamus, and internal capsule), comprises no more than half of all ICH cases.³² Basic research translation to clinical studies has given little attention to posterior stroke.^{17,18,34,41,80} The duality of being too uncommon to achieve sufficient numbers in some patient centers, confounded by clinicopathological heterogeneity³⁹ between posterior and anterior circulation stroke, makes experimental models representing this condition all the more needed. Animal models representing the full spectrum of ICH are thus needed.^{70,116}

Over the past half century, surgical approaches for brainstem hemorrhages have been widely debated in the literature.^{6,46,54,55,57,58,61,83,86,89,90,96,118} In fact, the report of successful pontine infusion into the rat pons tegmentum was what first prompted the development of this model.⁹¹ However, this infratentorial (pontine hemorrhage) patient population has been

excluded from what will arguably be one of the greatest pivotal clinical studies on surgical treatment of ICH in a decade.^{79,80} Furthermore, this study is an extension of our infratentorial hemorrhage rodent studies of the cerebellum^{64,65} and builds on our preliminary report describing the feasibility of experimental pontine hemorrhage.⁶⁶ Early outcomes after pontine hemorrhage are dependent on the extent of the initial bleed^{85,127} more than anything else.⁹ The use of collagenase thus relates well to the study of the human clinical PPH condition,⁷⁸ because many have reproducibly demonstrated the utility of collagenase in the evaluation of strategies to mitigate early hematoma expansion.¹⁰⁴ The clinical relevance of this animal model relates to the fact that pontine hemorrhage represents such a small percentage of ICH—thus making high-quality clinical studies difficult to perform and highlighting the need of an instructive animal model to evaluate strategies to prevent and treat posthemorrhagic complications.

The early hematoma consequences in the present study were in agreement with experimental findings of basal ganglia ICH in rats with regard to collagenase-induced edema, neurodeficit, blood-brain barrier rupture, and elevation of MMP-2 and -9 levels.^{100,106,126} Our immunoblots demonstrated relative changes in the protein expression of MMP subtypes, while further study using gel zymography will define the change in MMP-2 and -9 enzymatic activity. In further limitation, future work will need to determine any temporally related changes to cortical cerebral blood flow, and intracranial pressures, just as these changes were determined following related experimental subarachnoid hemorrhage in rats.⁵¹ Nonetheless, this model demonstrated consistent neurobehavioral outcomes using 0.15-0.3 U of collagenase, much like the basal ganglia ICH using 0.2 U of collagenase in rats.⁷¹ This is well below the amount known to cause significant neurotoxicity.⁷⁶ Thus, both doses of collagenase produced adequate neurological injury, and we chose the lower dose for long-term evaluations. This minimized any additional collagenase contribution to inflammation¹²⁵ and also prevented any component of vestibular syndrome (head tilt or rolling) at the 30-day evaluation. The robust performance of lesioned animals in finding the platform in the cued water maze trials confirmed the lack of any significant visual-vestibular disturbance. On the other hand, the infusion of collagenase is likely to ultimately affect both the composition of the extracellular matrix and the migration of inflammatory cells. This may therefore limit the use of this model to explore treatments aimed at modulating the inflammatory response after pontine hemorrhage. Future studies may therefore evaluate additional molecular mechanisms as interventional strategies for the early hematoma, neurobehavioral deficits, and neurovascular remodeling.^{106,132,135}

Importantly, the collagenase infusion yielded long-term neurobehavioral patterns similar to clinical reports after survivable pontine hemorrhage in humans.^{22,127} Almost one-half of survivors from pontine hemorrhage will retain long-term deficits across motor-learning and visuospatial neurocognitive domains, even after full rehabilitation from paralytic losses of overall strength, muscle tone, and coordination.^{74,75,88} In agreement, our study demonstrated that most neurological impairments resolved over the first 3 weeks of assessments, while motor-learning (rotarod) and cognitive ability (water maze and T-maze) remained impaired up to 1 month later. Similar neurobehavioral outcomes were confirmed, having been described in other experimental brainstem lesion models using rats.^{23,36,40,115,122} Interestingly, the finding of marginal (inclined-plane) hindlimb recovery diverged from both clinical and previously known experimental manifestations. This is possibly a rodent (and model)-specific feature, since the lateral placement of our 30-day ventral pontine tegmentum lesion anatomically obliterates the rodent hindlimb control region, while the forelimb neuronal tracts are located more medially in the rodent brainstem.^{81,107} Also, the lateral pons-brainstem contains cerebropontocerebellar projections that link hindlimb control regions of the cerebral cortex and cerebellum together to form the largest sensorimotor structure within the mammalian brain.⁹² Therefore any obliteration

along these neural tracts could lead to lasting hindlimb deficits, similar to those found after cerebellar hemorrhage in rats.⁶⁴

As previously mentioned, there have been several prior reports about cognitive deficits following infratentorial lesions, and the topic of clinically translating such data has been extensively reviewed.^{42,63,64,67,104} Notwithstanding, clinical cognitive dysfunction following brainstem hemorrhage in humans remains a weakly reported fact in the literature,^{74,88} and our study further highlights the novelty and importance of using such a rodent ICH model to examine an important clinical outcome of which little is known.²² However, in terms of specifically why cognitive deficits were observed following pontine hemorrhage, one can only speculate. Although we were not surprised to find that pontine lesions were associated with sensorimotor, coordination, and motor-learning deficits (as seen in the rotarod), we acknowledge that finding cognitive deficits following a pontine lesion was unexpected. Nevertheless, the animals generally appeared normal while walking or swimming, and we are confident that the deficits described were due to cognitive, rather than sensorimotor and/or coordination, issues. First, the cued task provides a built-in behavioral control for the water maze test.⁴³ The observation that all groups performed equally when the escape platform was visible suggests that all groups were equally motivated to find the platform, that they could see the platform, and that they could easily swim to the platform. Only when the platform was submerged (requiring the use relational/contextual learning strategies) did the behavior of the pons group decline. This pattern of activity (unimpaired cued behavior with a visible platform, but impaired performance with a hidden platform) represents the classic spatial-learning deficit.⁸⁴ Second, also during the probe tasks in which the platform was removed, only the pontine group swam randomly around the tank, whereas only the control groups exhibited targeted searches in the quadrant that previously contained the platform. Again, this pattern of behavior is representative of the classic spatial memory deficit.⁴⁴ Third, during these probe trials, all groups swam at a similar speed and covered a similar distance, signifying the lack of neurological-functional differences between the groups for this specific task. The finding of impaired working memory performance on the T-maze task further supports this interpretation, because walking down the T-maze was easy enough for all rats and yet only the pontine group exhibited random performance, which is classically interpreted, in the absence of any overt motor issues that would inhibit performance, as an impaired working memory.²⁸

The neuropathology after pontine hemorrhage has been poorly described, but it is necessary for the establishment of the therapeutic window and for the choice of drug. Therefore, we related our neurological outcomes with the histopathological substrates, as a morphological measure of the brain injury.^{29,48} Thirty days after collagenase infusion, we found a well-circumscribed atrophic cavitory lesion in the right pons-brainstem. The atrophy was focal (nonspreading), not significantly affecting the rostral (midbrain), caudal (medulla), or dorsal (cerebellar hemisphere) structures. Such focal cystic cavitory lesions similarly occur after experimental basal ganglia ICH in rats.^{29,71} However, we did find diffuse (nonfocal) losses of neuronal density in the midbrain, pontine, and medulla 1 month after collagenase infusion (0.15 U). These neuronal tissue losses likely contributed to the causation of delayed neurocognitive and hindlimb deficits. Further studies will need to investigate the involvement of specific nuclei or fascicles, to describe the key structures involved in the pons, and the related anatomical areas in the brainstem and in the cerebellum—to specifically describe which structures were destroyed, which nucleus lost its neurons, and which fascicles degenerated. There is a need to evaluate the role of neuronal apoptosis, the possible timelines of Wallerian degeneration, and the pattern of inflammation and astrogliosis. Taken together, the combined networks of linked neuropathological injuries after pontine hemorrhage represent potential treatable lesions using therapeutic neuroprotective strategies.¹¹⁰

To date, all the preclinical ICH studies to improve functional outcome have been performed using models of basal ganglia hemorrhage, and these interventions have been extensively reviewed in a recent meta-analysis.³⁵ An impressively scant amount is known about the brainstem with regard to potentials in neuroprotection, neuroplasticity, and the utility of stem cells or pharmacological approaches.^{25,72,73} To highlight the differences, compared with the more common basal ganglia hemorrhages (ICH) having less than 50% mortality rates,⁷ PPH is highly lethal, leading to a mortality rate in excess of 65%.^{15,31,137} This much greater severity is likely related to the many ascending and descending brainstem projections connected with the reticular formation, cardiovascular, and respiratory centers (reviewed by Lekic et al.⁶³). Current therapeutic approaches following PPH, however, are largely based on outcomes found in basal ganglia hemorrhage.^{72,73} Comparatively, whereas up to 80% of rehabilitating ICH patients are not yet living independently by 6 months following stroke, ³⁷ deficits in most PPH events are so severe that the majority of patients may not even qualify to enter rehabilitation because of such a poor prognosis and survival rate.¹⁰⁸ As the basis for this and future research, this PPH animal model can relevantly address the goals of clinically improving the rates of mortality, overall morbidity, and ultimate functional recovery using future experimental studies.

Brainstem nuclei are anatomically scattered in a mosaic of physiologically relevant neuronal islands.^{2,5,94,103,120} A gerbil model of hindbrain ischemia has shown the greatest numbers of cell deaths near areas of coordination and balance (cerebellar interpositus and lateral vestibular nuclei) while cardiorespiratory foci had seemingly greater “innate” neuroprotection.⁴⁵ Similarly, our study found lasting neurobehavioral deficits, while (cardiorespiratory) physiological variables remained intact up to 30 days later. Loss of these life-sustaining nuclei may, however, explain our 30-day mortality rate (approximately 50%), which is analogous to the clinical findings.¹³⁷ Clinically, brainstem neurons located within the area postrema contribute important regulations in terms of cardiovascular functions.^{53,101,112,134} This brain region expresses cell-surface receptors for circulating molecules (angiotensin II and vasopressin), and likely has some control over cerebrovascular activity.^{38,49,68} In the brainstem, the angiotensin II hormone resets the baroreflex to a higher blood pressure level through indirect interactions with the solitary tract nucleus and through interconnections to the medulla.^{77,95,131} These nuclei also modulate the cardiovascular regulation of other neuropeptides, such as vasopressin; this homeostatic effector can readily bind to somatic V2-type receptors, causing peripheral vasoconstriction. On the other hand, vasopressin receptor binding interactions at the area postrema will paradoxically enhance the baroreflex set-point to an activation level of lower threshold pressure.^{20,59,93} Experimental studies further reveal significant cerebellar fastigial nuclei involvement in this cerebrovascular control.^{69,82,130} The interaction occurs through an integration of autonomic signals arising from adjacent brainstem vestibular and Purkinje neurons.^{24,133} As part of a larger brainstem network, the cerebellar fastigial nuclei modulate function of medullary structures and autonomic spinal intermediolateral column neurons.^{11,21} In primates, these nuclei circuits are pathways to interconnect the vestibular (lateral and inferior), reticular (lateral, paramedian, and gigantocellular), and cervical spinal anterior gray neurons.⁴ Depending on the type of infratentorial brain injury, experimental studies have demonstrated that electrical stimulation of the fastigial nuclei leads to pressor responses with tachycardia (mediated by fibers passing through, or very close to, the nuclei), while chemical activation causes bradycardia depressor responses through intrinsic fastigial nuclei neuronal activity.^{12,13,97} Taken together, these clinically relevant human infratentorial circuitry pathways help keep the balance of complex cerebrovascular systems and underscore the importance of better understanding localized lesions to this brain region. This experimental PPH model thus represents a means of impacting future patient care through the study of specific surgical, pharmacological, and regenerative approaches.

Conclusions

We have characterized the early brain injury, neurobehavioral profiles, and histopathology in a highly reliable and easily reproducible experimental model of pontine hemorrhage using rats. Therapeutic strategies that mitigate the early mass effect (hematoma growth and brain edema), or promote lasting neuroprotection (neurobehavioral and atrophic remodeling) could lead to clinical approaches that afford these patients better outcomes in the future.^{102,124,129} While the present study has well characterized the neurological deficits, particularly during the chronic phase, pathophysiological investigations are needed to help establish the therapeutic window for mitigating early (and delayed) damage, the choice of drugs, and the appropriate design of stroke rehabilitation studies. These findings provide a basis for the establishment of these pathophysiological features, serving as a foundation on which to perform further therapeutic investigation.

Acknowledgments

The authors thank Suzzanne Marcantonio for technical assistance with the physiological monitoring equipment.

Contract grant sponsorship was received from NIH: nos. HD43120 (to J.H.Z.), NS43338 (to J.H.Z.), and NS54685 (to J.H.Z.).

Abbreviations used in this paper

ICH	intracerebral hemorrhage
PBS	phosphate-buffered saline
PPH	primary pontine hemorrhage

References

1. Andaluz N, Zuccarello M, Wagner KR. Experimental animal models of intracerebral hemorrhage. *Neurosurg Clin N Am.* 2002; 13:385–393. [PubMed: 12486927]
2. Avendaño C, Machín R, Bermejo PE, Lagares A. Neuron numbers in the sensory trigeminal nuclei of the rat: A GABA- and glycine-immunocytochemical and stereological analysis. *J Comp Neurol.* 2005; 493:538–553. [PubMed: 16304625]
3. Balci K, Asil T, Kerimoglu M, Celik Y, Utku U. Clinical and neuroradiological predictors of mortality in patients with primary pontine hemorrhage. *Clin Neurol Neurosurg.* 2005; 108:36–39. [PubMed: 16311143]
4. Batton RR III, Jayaraman A, Ruggiero D, Carpenter MB. Fastigial efferent projections in the monkey: an autoradiographic study. *J Comp Neurol.* 1977; 174:281–305. [PubMed: 68041]
5. Bermejo PE, Jiménez CE, Torres CV, Avendaño C. Quantitative stereological evaluation of the gracile and cuneate nuclei and their projection neurons in the rat. *J Comp Neurol.* 2003; 463:419–433. [PubMed: 12836177]
6. Bosch DA, Beute GN. Successful stereotaxic evacuation of an acute pontomedullary hematoma. Case report. *J Neurosurg.* 1985; 62:153–156. [PubMed: 3880583]
7. Broderick JP, Adams HP Jr, Barsan W, Feinberg W, Feldmann E, Grotta J, et al. Guidelines for the management of spontaneous intracerebral hemorrhage: a statement for healthcare professionals from a special writing group of the Stroke Council, American Heart Association. *Stroke.* 1999; 30:905–915. [PubMed: 10187901]
8. Broderick JP, Brott TG, Duldner JE, Tomsick T, Huster G. Volume of intracerebral hemorrhage. A powerful and easy-to-use predictor of 30-day mortality. *Stroke.* 1993; 24:987–993. [PubMed: 8322400]

9. Broderick JP, Diringer MN, Hill MD, Brun NC, Mayer SA, Steiner T, et al. Determinants of intracerebral hemorrhage growth: an exploratory analysis. *Stroke*. 2007; 38:1072–1075. [PubMed: 17290026]
10. Burns J, Lisak R, Schut L, Silberberg D. Recovery following brainstem hemorrhage. *Ann Neurol*. 1980; 7:183–184. [PubMed: 7369723]
11. Caverson MM, Ciriello J, Calaresu FR. Direct pathway from cardiovascular neurons in the ventrolateral medulla to the region of the intermediolateral nucleus of the upper thoracic cord: an anatomical and electrophysiological investigation in the cat. *J Auton Nerv Syst*. 1983; 9:451–475. [PubMed: 6363504]
12. Chida K, Iadecola C, Reis DJ. Lesions of rostral ventrolateral medulla abolish some cardio- and cerebrovascular components of the cerebellar fastigial pressor and depressor responses. *Brain Res*. 1990; 508:93–104. [PubMed: 2337796]
13. Chida K, Iadecola C, Underwood MD, Reis DJ. A novel vasodepressor response elicited from the rat cerebellar fastigial nucleus: the fastigial depressor response. *Brain Res*. 1986; 370:378–382. [PubMed: 3708335]
14. Choudhri TF, Hoh BL, Solomon RA, Connolly ES Jr, Pinsky DJ. Use of a spectrophotometric hemoglobin assay to objectively quantify intracerebral hemorrhage in mice. *Stroke*. 1997; 28:2296–2302. [PubMed: 9368579]
15. Chung CS, Park CH. Primary pontine hemorrhage: a new CT classification. *Neurology*. 1992; 42:830–834. [PubMed: 1565238]
16. Chung Y, Haines SJ. Experimental brain stem surgery. *Neurosurg Clin N Am*. 1993; 4:405–414. [PubMed: 8353441]
17. Clark WM, Albers GW, Madden KP, Hamilton S. The rtPA (alteplase) 0- to 6-hour acute stroke trial, part A (A0276g): results of a double-blind, placebo-controlled, multicenter study. *Stroke*. 2000; 31:811–816. [PubMed: 10753980]
18. Clark WM, Wissman S, Albers GW, Jhamandas JH, Madden KP, Hamilton S. Recombinant tissue-type plasminogen activator (Alteplase) for ischemic stroke 3 to 5 hours after symptom onset. *JAMA*. 1999; 282:2019–2026. [PubMed: 10591384]
19. Colombel C, Lalonde R, Caston J. The effects of unilateral removal of the cerebellar hemispheres on motor functions and weight gain in rats. *Brain Res*. 2002; 950:231–238. [PubMed: 12231248]
20. Cox BF, Hay M, Bishop VS. Neurons in area postrema mediate vasopressin-induced enhancement of the baroreflex. *Am J Physiol*. 1990; 258:H1943–H1946. [PubMed: 2360682]
21. Dampney RA, Goodchild AK, Robertson LG, Montgomery W. Role of ventrolateral medulla in vasomotor regulation: a correlative anatomical and physiological study. *Brain Res*. 1982; 249:223–235. [PubMed: 6128058]
22. Del Brutto OH, Campos X. Validation of intracerebral hemorrhage scores for patients with pontine hemorrhage. *Neurology*. 2004; 62:515–516. [PubMed: 14872050]
23. Dellu F, Mayo W, Cherkaoui J, Le Moal M, Simon H. Learning disturbances following excitotoxic lesion of cholinergic pedunculo-pontine nucleus in the rat. *Brain Res*. 1991; 544:126–132. [PubMed: 1855131]
24. Doba N, Reis DJ. Role of the cerebellum and the vestibular apparatus in regulation of orthostatic reflexes in the cat. *Circ Res*. 1974; 40:9–18. [PubMed: 4543723]
25. Donnan GA, Fisher M, Macleod M, Davis SM. *Stroke*. *Lancet*. 2008; 371:1612–1623. [PubMed: 18468545]
26. Dziewas R, Kremer M, Lüdemann P, Nabavi DG, Dräger B, Ringelstein B. The prognostic impact of clinical and CT parameters in patients with pontine hemorrhage. *Cerebrovasc Dis*. 2003; 16:224–229. [PubMed: 12865609]
27. Ekinçi N, Acer N, Akkaya A, Sankur S, Kabadayi T, Sahin B. Volumetric evaluation of the relations among the cerebrum, cerebellum and brain stem in young subjects: a combination of stereology and magnetic resonance imaging. *Surg Radiol Anat*. 2008; 30:489–494. [PubMed: 18478176]
28. Fathali N, Ostrowski RP, Lekic T, Jadhav V, Tong W, Tang J, et al. Cyclooxygenase-2 inhibition provides lasting protection against neonatal hypoxic-ischemic brain injury. *Crit Care Med*. 2010; 38:572–578. [PubMed: 20029340]

29. Felberg RA, Grotta JC, Shirzadi AL, Strong R, Narayana P, Hill-Felberg SJ, et al. Cell death in experimental intracerebral hemorrhage: the “black hole” model of hemorrhagic damage. *Ann Neurol.* 2002; 51:517–524. [PubMed: 11921058]
30. Fernandez AM, de la Vega AG, Torres-Aleman I. Insulin-like growth factor I restores motor coordination in a rat model of cerebellar ataxia. *Proc Natl Acad Sci U S A.* 1998; 95:1253–1258. [PubMed: 9448318]
31. Flaherty ML, Haverbusch M, Sekar P, Kissela B, Kleindorfer D, Moomaw CJ, et al. Long-term mortality after intracerebral hemorrhage. *Neurology.* 2006; 66:1182–1186. [PubMed: 16636234]
32. Flaherty ML, Woo D, Haverbusch M, Sekar P, Khoury J, Sauerbeck L, et al. Racial variations in location and risk of intracerebral hemorrhage. *Stroke.* 2005; 36:934–937. [PubMed: 15790947]
33. Foerch C, Arai K, Jin G, Park KP, Pallast S, van Leyen K, et al. Experimental model of warfarin-associated intracerebral hemorrhage. *Stroke.* 2008; 39:3397–3404. [PubMed: 18772448]
34. Foulkes MA, Wolf PA, Price TR, Mohr JP, Hier DB. The Stroke Data Bank: design, methods, and baseline characteristics. *Stroke.* 1988; 19:547–554. [PubMed: 3363586]
35. Frantzas J, Sena ES, Macleod MR, Al-Shahi Salman R. Treatment of intracerebral hemorrhage in animal models: meta-analysis. *Ann Neurol.* 2011; 69:389–399. [PubMed: 21387381]
36. Gasbarri A, Pompili A, Pacitti C, Cicirata F. Comparative effects of lesions to the ponto-cerebellar and olivo-cerebellar pathways on motor and spatial learning in the rat. *Neuroscience.* 2003; 116:1131–1140. [PubMed: 12617954]
37. Gebel JM, Broderick JP. Intracerebral hemorrhage. *Neurol Clin.* 2000; 18:419–438. [PubMed: 10757834]
38. Gerstberger R, Fahrenholz F. Autoradiographic localization of V1 vasopressin binding sites in rat brain and kidney. *Eur J Pharmacol.* 1989; 167:105–116. [PubMed: 2528467]
39. Goto N, Kaneko M, Hosaka Y, Koga H. Primary pontine hemorrhage: clinicopathological correlations. *Stroke.* 1980; 11:84–90. [PubMed: 7355436]
40. Grillner S, Wallen P, Saitoh K, Kozlov A, Robertson B. Neural bases of goal-directed locomotion in vertebrates—an overview. *Brain Res Rev.* 2008; 57:2–12. [PubMed: 17916382]
41. Hacke W, Kaste M, Fieschi C, Toni D, Lesaffre E, von Kummer R, et al. Intravenous thrombolysis with recombinant tissue plasminogen activator for acute hemispheric stroke. *JAMA.* 1995; 274:1017–1025. [PubMed: 7563451]
42. Hartman R, Lekic T, Rojas H, Tang J, Zhang JH. Assessing functional outcomes following intracerebral hemorrhage in rats. *Brain Res.* 2009; 1280:148–157. [PubMed: 19464275]
43. Hartman RE, Izumi Y, Bales KR, Paul SM, Wozniak DF, Holtzman DM. Treatment with an amyloid-beta antibody ameliorates plaque load, learning deficits, and hippocampal long-term potentiation in a mouse model of Alzheimer’s disease. *J Neurosci.* 2005; 25:6213–6220. [PubMed: 15987951]
44. Hartman RE, Shah A, Fagan AM, Schwetye KE, Parsadanian M, Schulman RN, et al. Pomegranate juice decreases amyloid load and improves behavior in a mouse model of Alzheimer’s disease. *Neurobiol Dis.* 2006; 24:506–515. [PubMed: 17010630]
45. Hata R, Matsumoto M, Hatakeyama T, Ohtsuki T, Handa N, Niinobe M, et al. Differential vulnerability in the hindbrain neurons and local cerebral blood flow during bilateral vertebral occlusion in gerbils. *Neuroscience.* 1993; 56:423–439. [PubMed: 8247270]
46. Hellwig D, Bertalanffy H, Bauer BL, Tirakotai W. Pontine hemorrhage. *J Neurosurg.* 2003; 99:796–797. Letter. [PubMed: 14567621]
47. Henninger N, Eberius KH, Sicard KM, Kollmar R, Sommer C, Schwab S, et al. A new model of thromboembolic stroke in the posterior circulation of the rat. *J Neurosci Methods.* 2006; 156:1–9. [PubMed: 16530271]
48. Hua Y, Schallert T, Keep RF, Wu J, Hoff JT, Xi G. Behavioral tests after intracerebral hemorrhage in the rat. *Stroke.* 2002; 33:2478–2484. [PubMed: 12364741]
49. Huang J, Hara Y, Anrather J, Speth RC, Iadecola C, Pickel VM. Angiotensin II subtype 1A (AT1A) receptors in the rat sensory vagal complex: subcellular localization and association with endogenous angiotensin. *Neuroscience.* 2003; 122:21–36. [PubMed: 14596846]

50. Hughes RN. The value of spontaneous alternation behavior (SAB) as a test of retention in pharmacological investigations of memory. *Neurosci Biobehav Rev.* 2004; 28:497–505. [PubMed: 15465137]
51. Jackowski A, Crockard A, Burnstock G, Russell RR, Kristek F. The time course of intracranial pathophysiological changes following experimental subarachnoid haemorrhage in the rat. *J Cereb Blood Flow Metab.* 1990; 10:835–849. [PubMed: 2211877]
52. Jeong JH, Yoon SJ, Kang SJ, Choi KG, Na DL. Hypertensive pontine microhemorrhage. *Stroke.* 2002; 33:925–929. [PubMed: 11935038]
53. Joy MD, Lowe RD. Evidence that the area postrema mediates the central cardiovascular response to angiotensin II. *Nature.* 1970; 228:1303–1304. [PubMed: 4321187]
54. Kanno T, Sano H, Shinomiya Y, Katada K, Nagata J, Hoshino M, et al. Role of surgery in hypertensive intracerebral hematoma. A comparative study of 305 nonsurgical and 154 surgical cases. *J Neurosurg.* 1984; 61:1091–1099. [PubMed: 6502238]
55. Kline DG, LeBlanc HJ. Survival following gunshot wound of the pons: neuroanatomic considerations. Case report. *J Neurosurg.* 1971; 35:342–347. [PubMed: 22046650]
56. Koliatsos VE, Cernak I, Xu L, Song Y, Savonenko A, Crain BJ, et al. A mouse model of blast injury to brain: initial pathological, neuropathological, and behavioral characterization. *J Neuropathol Exp Neurol.* 2011; 70:399–416. [PubMed: 21487304]
57. Konovalov AN, Spallone A, Makhmudov UB, Kukhlajeva JA, Ozerova VI. Surgical management of hematomas of the brain stem. *J Neurosurg.* 1990; 73:181–186. [PubMed: 2366074]
58. Koos WT, Sunder-Plassmann M, Salah S. Successful removal of a large intrapontine hematoma. Case report. *J Neurosurg.* 1969; 31:690–694. [PubMed: 5359217]
59. Koshimizu TA, Nasa Y, Tanoue A, Oikawa R, Kawahara Y, Kiyono Y, et al. V1a vasopressin receptors maintain normal blood pressure by regulating circulating blood volume and baroreflex sensitivity. *Proc Natl Acad Sci U S A.* 2006; 103:7807–7812. [PubMed: 16682631]
60. Kushner MJ, Bressman SB. The clinical manifestations of pontine hemorrhage. *Neurology.* 1985; 35:637–643. [PubMed: 3990963]
61. Kyoshima K, Kobayashi S, Gibo H, Kuroyanagi T. A study of safe entry zones via the floor of the fourth ventricle for brainstem lesions. Report of three cases. *J Neurosurg.* 1993; 78:987–993. [PubMed: 8487085]
62. Lekic T, Hartman R, Rojas H, Manaenko A, Chen W, Ayer R, et al. Protective effect of melatonin upon neuropathology, striatal function, and memory ability after intracerebral hemorrhage in rats. *J Neurotrauma.* 2010; 27:627–637. [PubMed: 20350200]
63. Lekic T, Krafft PR, Coats JS, Obenaus A, Tang J, Zhang JH. Infratentorial strokes for posterior circulation folks: clinical correlations for current translational therapeutics. *Transl Stroke Res.* 2011; 2:144–151. [PubMed: 23060944]
64. Lekic T, Rolland W, Hartman R, Kamper J, Suzuki H, Tang J, et al. Characterization of the brain injury, neurobehavioral profiles, and histopathology in a rat model of cerebellar hemorrhage. *Exp Neurol.* 2011; 227:96–103. [PubMed: 20887722]
65. Lekic T, Tang J, Zhang JH. Rat model of intracerebellar hemorrhage. *Acta Neurochir Suppl.* 2008; 105:131–134. [PubMed: 19066098]
66. Lekic T, Tang J, Zhang JH. A rat model of pontine hemorrhage. *Acta Neurochir Suppl.* 2008; 105:135–137. [PubMed: 19066099]
67. Lekic T, Zhang JH. Posterior circulation stroke and animal models. *Front Biosci.* 2008; 13:1827–1844. [PubMed: 17981671]
68. Lenkei Z, Palkovits M, Corvol P, Llorens-Cortès C. Expression of angiotensin type-1 (AT1) and type-2 (AT2) receptor mRNAs in the adult rat brain: a functional neuroanatomical review. *Front Neuroendocrinol.* 1997; 18:383–439. [PubMed: 9344632]
69. Lutherer LO, Lutherer BC, Dormer KJ, Janssen HF, Barnes CD. Bilateral lesions of the fastigial nucleus prevent the recovery of blood pressure following hypotension induced by hemorrhage or administration of endotoxin. *Brain Res.* 1983; 269:251–257. [PubMed: 6349747]
70. MacLellan CL, Silasi G, Auriat AM, Colbourne F. Rodent models of intracerebral hemorrhage. *Stroke.* 2010; 41(10 Suppl):S95–S98. [PubMed: 20876518]

71. MacLellan CL, Silasi G, Poon CC, Edmundson CL, Buist R, Peeling J, et al. Intracerebral hemorrhage models in rat: comparing collagenase to blood infusion. *J Cereb Blood Flow Metab.* 2008; 28:516–525. [PubMed: 17726491]
72. Macleod M. Current issues in the treatment of acute posterior circulation stroke. *CNS Drugs.* 2006; 20:611–621. [PubMed: 16863267]
73. Macleod MR, Davis SM, Mitchell PJ, Gerraty RP, Fitt G, Hankey GJ, et al. Results of a multicentre, randomised controlled trial of intra-arterial urokinase in the treatment of acute posterior circulation ischaemic stroke. *Cerebrovasc Dis.* 2005; 20:12–17. [PubMed: 15925877]
74. Maeshima S, Osawa A, Kunishio K. Cognitive dysfunction in a patient with brainstem hemorrhage. *Neurol Sci.* 2010; 31:495–499. [PubMed: 20229078]
75. Masiyama S, Niizuma H, Suzuki J. Pontine haemorrhage: a clinical analysis of 26 cases. *J Neurol Neurosurg Psychiatry.* 1985; 48:658–662. [PubMed: 4031910]
76. Matsushita K, Meng W, Wang X, Asahi M, Asahi K, Moskowitz MA, et al. Evidence for apoptosis after intercerebral hemorrhage in rat striatum. *J Cereb Blood Flow Metab.* 2000; 20:396–404. [PubMed: 10698078]
77. McMullan S, Goodchild AK, Pilowsky PM. Circulating angiotensin II attenuates the sympathetic baroreflex by reducing the barosensitivity of medullary cardiovascular neurones in the rat. *J Physiol.* 2007; 582:711–722. [PubMed: 17363385]
78. Meenakshi-Sundaram S, Anand TC, Suriyakumar G, Sridhar R, Sundararajan S, Sundar B. Recombinant factor VIIa in a case of pontine hemorrhage. *J Assoc Physicians India.* 2008; 56:719–720. [PubMed: 19086362]
79. Mendelow AD, Gregson BA, Fernandes HM, Murray GD, Teasdale GM, Hope DT, et al. Early surgery versus initial conservative treatment in patients with spontaneous supratentorial intracerebral haematomas in the International Surgical Trial in Intracerebral Haemorrhage (STICH): a randomised trial. *Lancet.* 2005; 365:387–397. [PubMed: 15680453]
80. Mendelow AD, Unterberg A. Surgical treatment of intracerebral haemorrhage. *Curr Opin Crit Care.* 2007; 13:169–174. [PubMed: 17327738]
81. Mileikovskii BYU, Kiyashchenko LI, Titkov ES. Changes in neuron activity in the dorsolateral part of the pons during stimulation of areas of the brainstem inhibiting movement and muscle tone. *Neurosci Behav Physiol.* 2001; 31:641–646. [PubMed: 11766905]
82. Miura M, Reis DJ. Cerebellum: a pressor response elicited from the fastigial nucleus and its efferent pathway in brainstem. *Brain Res.* 1969; 13:595–599. [PubMed: 5772438]
83. Miyagi Y, Shima F, Ishido K, Moriguchi M, Kamikaseda K. Posteroventral pallidotomy for midbrain tremor after a pontine hemorrhage. Case report. *J Neurosurg.* 1999; 91:885–888. [PubMed: 10541252]
84. Morris RG, Garrud P, Rawlins JN, O'Keefe J. Place navigation impaired in rats with hippocampal lesions. *Nature.* 1982; 297:681–683. [PubMed: 7088155]
85. Murata Y, Yamaguchi S, Kajikawa H, Yamamura K, Sumioka S, Nakamura S. Relationship between the clinical manifestations, computed tomographic findings and the outcome in 80 patients with primary pontine hemorrhage. *J Neurol Sci.* 1999; 167:107–111. [PubMed: 10521548]
86. Murphy MG. Successful evacuation of acute pontine hematoma. Case report. *J Neurosurg.* 1972; 37:224–225. [PubMed: 4558255]
87. NINDS ICH Workshop Participants. Priorities for clinical research in intracerebral hemorrhage: report from a National Institute of Neurological Disorders and Stroke workshop. *Stroke.* 2005; 36:e23–e41. [PubMed: 15692109]
88. Nys GM, van Zandvoort MJ, de Kort PL, Jansen BP, de Haan EH, Kappelle LJ. Cognitive disorders in acute stroke: prevalence and clinical determinants. *Cerebrovasc Dis.* 2007; 23:408–416. [PubMed: 17406110]
89. O'Laoire SA, Crockard HA, Thomas DG, Gordon DS. A report of six surgically treated cases. *J Neurosurg.* 1982; 56:222–227. [PubMed: 7054431]
90. Obrador S, Dierssen G, Odoriz BJ. Surgical evacuation of a pontine-medullary hematoma. Case report. *J Neurosurg.* 1970; 33:82–84. [PubMed: 5310588]
91. Occhiogrosso G, Edgar MA, Sandberg DI, Souweidane MM. Prolonged convection-enhanced delivery into the rat brainstem. *Neurosurgery.* 2003; 52:388–394. [PubMed: 12535369]

92. Odeh F, Ackerley R, Bjaalie JG, Apps R. Pontine maps linking somatosensory and cerebellar cortices are in register with climbing fiber somatotopy. *J Neurosci*. 2005; 25:5680–5690. [PubMed: 15958734]
93. Oikawa R, Nasa Y, Ishii R, Kuwaki T, Tanoue A, Tsujimoto G, et al. Vasopressin VIA receptor enhances baroreflex via the central component of the reflex arc. *Eur J Pharmacol*. 2007; 558:144–150. [PubMed: 17224142]
94. Oorschot DE. Total number of neurons in the neostriatal, pallidal, subthalamic, and substantia nigral nuclei of the rat basal ganglia: a stereological study using the cavalieri and optical disector methods. *J Comp Neurol*. 1996; 366:580–599. [PubMed: 8833111]
95. Osborn JW, Fink GD, Sved AF, Toney GM, Raizada MK. Circulating angiotensin II and dietary salt: converging signals for neurogenic hypertension. *Curr Hypertens Rep*. 2007; 9:228–235. [PubMed: 17519130]
96. Paillas JE, Alliez B. Surgical treatment of spontaneous intracerebral hemorrhage. Immediate and long-term results in 250 cases. *J Neurosurg*. 1973; 39:145–151. [PubMed: 4719694]
97. Parry TJ, McElligott JG. Kainic acid administration in the fastigial nucleus produces differential cardiovascular effects in awake and anesthetized rats. *Brain Res*. 1994; 635:27–36. [PubMed: 8173964]
98. Payne HA, Maravilla KR, Levinstone A, Heuter J, Tindall RS. Recovery from primary pontine hemorrhage. *Ann Neurol*. 1978; 4:557–558. [PubMed: 742855]
99. Peeling J, Del Bigio MR, Corbett D, Green AR, Jackson DM. Efficacy of disodium 4-[(tert-butylimino)methyl] benzene-1,3-disulfonate N-oxide (NXY-059), a free radical trapping agent, in a rat model of hemorrhagic stroke. *Neuropharmacology*. 2001; 40:433–439. [PubMed: 11166336]
100. Power C, Henry S, Del Bigio MR, Larsen PH, Corbett D, Imai Y, et al. Intracerebral hemorrhage induces macrophage activation and matrix metalloproteinases. *Ann Neurol*. 2003; 53:731–742. [PubMed: 12783419]
101. Price CJ, Hoyda TD, Ferguson AV. The area postrema: a brain monitor and integrator of systemic autonomic state. *Neuroscientist*. 2008; 14:182–194. [PubMed: 18079557]
102. Qureshi AI, Mendelow AD, Hanley DF. Intracerebral haemorrhage. *Lancet*. 2009; 373:1632–1644. [PubMed: 19427958]
103. Reisert I, Wildemann G, Grab D, Pilgrim C. The glial reaction in the course of axon regeneration: a stereological study of the rat hypoglossal nucleus. *J Comp Neurol*. 1984; 229:121–128. [PubMed: 6490973]
104. Rosenberg GA. Modeling of cerebellar hemorrhage. *Exp Neurol*. 2011; 228:157–159. [PubMed: 21192929]
105. Rosenberg GA, Mun-Bryce S, Wesley M, Kornfeld M. Collagenase-induced intracerebral hemorrhage in rats. *Stroke*. 1990; 21:801–807. [PubMed: 2160142]
106. Rosenberg GA, Navratil M. Metalloproteinase inhibition blocks edema in intracerebral hemorrhage in the rat. *Neurology*. 1997; 48:921–926. [PubMed: 9109878]
107. Ross GS, Sinnamoni HM. Forelimb and hindlimb stepping by the anesthetized rat elicited by electrical stimulation of the pons and medulla. *Physiol Behav*. 1984; 33:201–208. [PubMed: 6505062]
108. Ruhland JL, van Kan PL. Medial pontine hemorrhagic stroke. *Phys Ther*. 2003; 83:552–566. [PubMed: 12775201]
109. Saria A, Lundberg JM. Evans blue fluorescence: quantitative and morphological evaluation of vascular permeability in animal tissues. *J Neurosci Methods*. 1983; 8:41–49. [PubMed: 6876872]
110. Schmammann JD, Ko R, MacMore J. The human basis pontis: motor syndromes and topographic organization. *Brain*. 2004; 127:1269–1291. [PubMed: 15128614]
111. Schmidt WM, Kraus C, Höger H, Hochmeister S, Oberndorfer F, Branka M, et al. Mutation in the *Scyl1* gene encoding amino-terminal kinase-like protein causes a recessive form of spinocerebellar neurodegeneration. *EMBO Rep*. 2007; 8:691–697. [PubMed: 17571074]
112. Sisó S, Jeffrey M, González L. Sensory circumventricular organs in health and disease. *Acta Neuropathol*. 2010; 120:689–705. [PubMed: 20830478]

113. Song S, Hua Y, Keep RF, Hoff JT, Xi G. A new hippocampal model for examining intracerebral hemorrhage-related neuronal death: effects of deferoxamine on hemoglobin-induced neuronal death. *Stroke*. 2007; 38:2861–2863. [PubMed: 17761912]
114. Steiner T, Bösel J. Options to restrict hematoma expansion after spontaneous intracerebral hemorrhage. *Stroke*. 2010; 41:402–409. [PubMed: 20044536]
115. Steiniger B, Kretschmer BD. Effects of ibotenate pedunculo-pontine tegmental nucleus lesions on exploratory behaviour in the open field. *Behav Brain Res*. 2004; 151:17–23. [PubMed: 15084417]
116. Stroke Therapy Academic Industry Roundtable. Recommendations for standards regarding preclinical neuroprotective and restorative drug development. *Stroke*. 1999; 30:2752–2758. [PubMed: 10583007]
117. Sutherland GR, Auer RN. Primary intracerebral hemorrhage. *J Clin Neurosci*. 2006; 13:511–517. [PubMed: 16769513]
118. Takimoto H, Iwaisako K, Kubo S, Yamanaka K, Karasawa J, Yoshimine T. Transaqueductal aspiration of pontine hemorrhage with the aid of a neuroendoscope. Technical note. *J Neurosurg*. 2003; 98:917–919. [PubMed: 12691423]
119. Tang J, Liu J, Zhou C, Alexander JS, Nanda A, Granger DN, et al. Mmp-9 deficiency enhances collagenase-induced intracerebral hemorrhage and brain injury in mutant mice. *J Cereb Blood Flow Metab*. 2004; 24:1133–1145. [PubMed: 15529013]
120. Tang Y, Lopez I, Baloh RW. Age-related change of the neuronal number in the human medial vestibular nucleus: a stereological investigation. *J Vestib Res*. 2001; 11:357–363. [PubMed: 12446961]
121. Thiex R, Mayfrank L, Rohde V, Gilsbach JM, Tsirka SA. The role of endogenous versus exogenous tPA on edema formation in murine ICH. *Exp Neurol*. 2004; 189:25–32. [PubMed: 15296833]
122. Vann SD. Gudden's ventral tegmental nucleus is vital for memory: re-evaluating diencephalic inputs for amnesia. *Brain*. 2009; 132:2372–2384. [PubMed: 19602577]
123. Voetsch B, DeWitt LD, Pessin MS, Caplan LR. Basilar artery occlusive disease in the New England Medical Center Posterior Circulation Registry. *Arch Neurol*. 2004; 61:496–504. [PubMed: 15096396]
124. Wagner KR. Modeling intracerebral hemorrhage: glutamate, nuclear factor-kappa B signaling and cytokines. *Stroke*. 2007; 38(2 Suppl):753–758. [PubMed: 17261732]
125. Wang J, Doré S. Inflammation after intracerebral hemorrhage. *J Cereb Blood Flow Metab*. 2007; 27:894–908. [PubMed: 17033693]
126. Wang J, Tsirka SE. Neuroprotection by inhibition of matrix metalloproteinases in a mouse model of intracerebral haemorrhage. *Brain*. 2005; 128:1622–1633. [PubMed: 15800021]
127. Wessels T, Möller-Hartmann W, Noth J, Klötzsch C. CT findings and clinical features as markers for patient outcome in primary pontine hemorrhage. *AJNR Am J Neuroradiol*. 2004; 25:257–260. [PubMed: 14970027]
128. Wijdicks EF, St Louis E. Clinical profiles predictive of outcome in pontine hemorrhage. *Neurology*. 1997; 49:1342–1346. [PubMed: 9371919]
129. Xi G, Keep RF, Hoff JT. Mechanisms of brain injury after intracerebral haemorrhage. *Lancet Neurol*. 2006; 5:53–63. [PubMed: 16361023]
130. Xu F, Zhou T, Gibson T, Frazier DT. Fastigial nucleus-mediated respiratory responses depend on the medullary gigantocellular nucleus. *J Appl Physiol*. 2001; 91:1713–1722. [PubMed: 11568155]
131. Xue B, Gole H, Pamidimukkala J, Hay M. Role of the area postrema in angiotensin II modulation of baroreflex control of heart rate in conscious mice. *Am J Physiol Heart Circ Physiol*. 2003; 284:H1003–H1007. [PubMed: 12446285]
132. Xue M, Mikliaeva EI, Casha S, Zygun D, Demchuk A, Yong VW. Improving outcomes of neuroprotection by minocycline: guides from cell culture and intracerebral hemorrhage in mice. *Am J Pathol*. 2010; 176:1193–1202. [PubMed: 20110416]
133. Yates BJ. Vestibular influences on the autonomic nervous system. *Ann N Y Acad Sci*. 1996; 781:458–473. [PubMed: 8694435]

134. Ylitalo P, Karppanen H, Paasonen MK. Is the area postrema a control center of blood pressure? *Nature*. 1974; 247:58–59. [PubMed: 4808944]
135. Zhao BQ, Tejima E, Lo EH. Neurovascular proteases in brain injury, hemorrhage and remodeling after stroke. *Stroke*. 2007; 38(2 Suppl):748–752. [PubMed: 17261731]
136. Zhou Y, Fathali N, Lekic T, Tang J, Zhang JH. Glibenclamide improves neurological function in neonatal hypoxia-ischemia in rats. *Brain Res*. 2009; 1270:131–139. [PubMed: 19306849]
137. Zia E, Engström G, Svensson PJ, Norrving B, Pessah-Rasmussen H. Three-year survival and stroke recurrence rates in patients with primary intracerebral hemorrhage. *Stroke*. 2009; 40:3567–3573. [PubMed: 19729603]
138. Zuccarello M, Fiore DL, Trincia G, De Caro R, Pardatscher K, Andrioli GC. Traumatic primary brain stem haemorrhage. A clinical and experimental study. *Acta Neurochir (Wien)*. 1983; 67:103–113. [PubMed: 6837339]

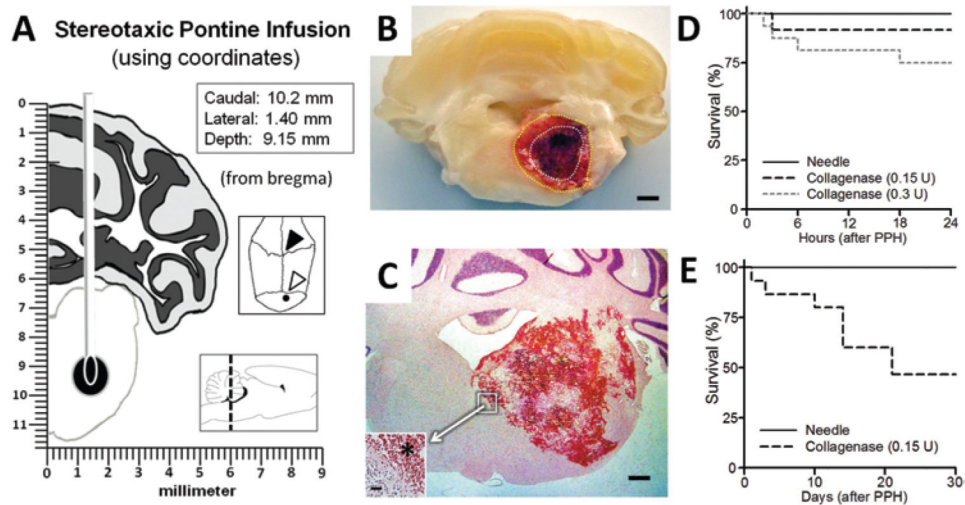
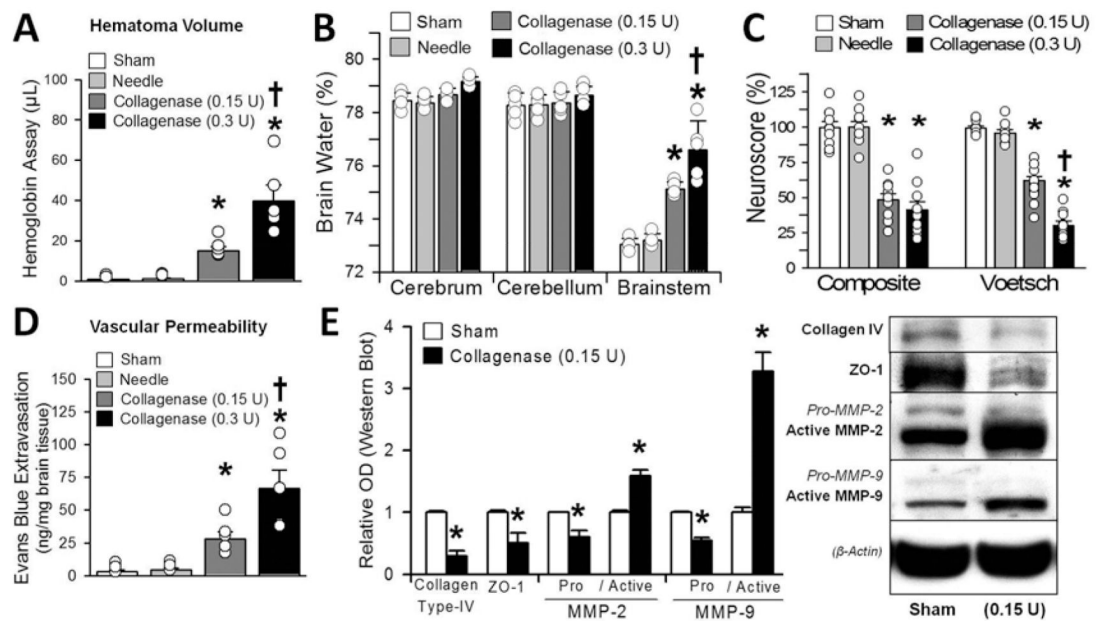
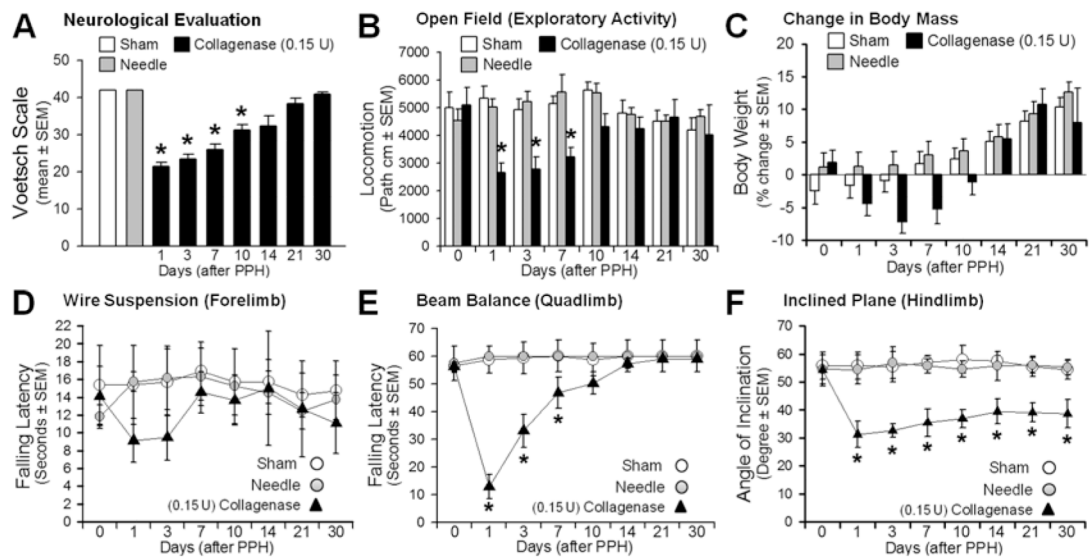


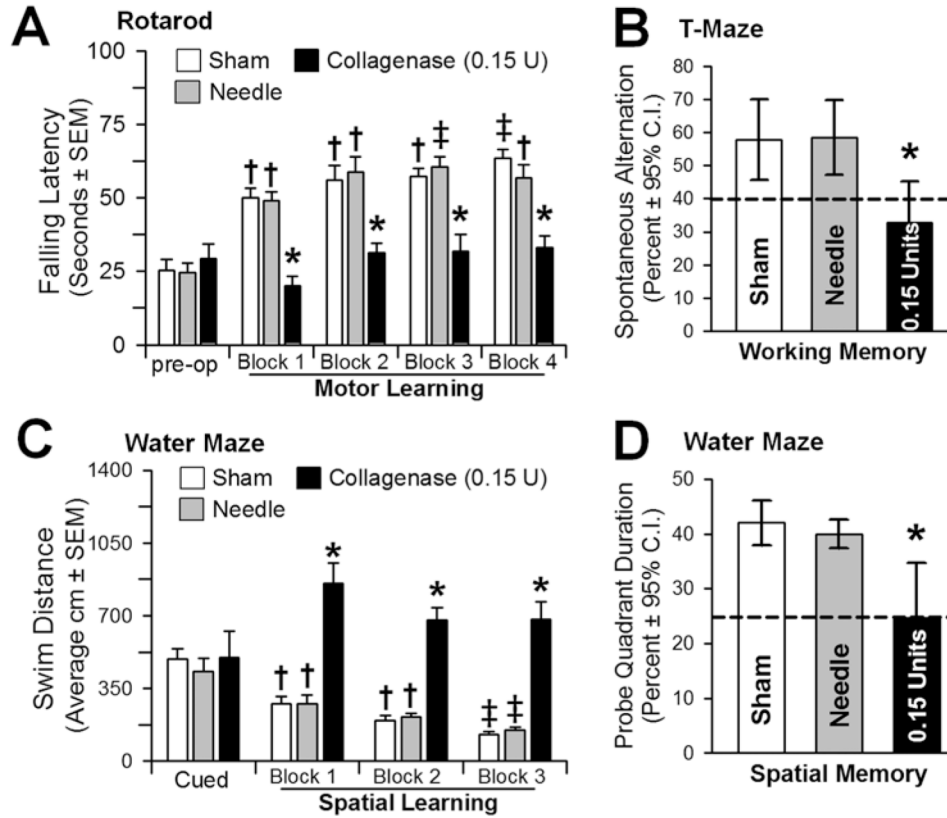
Fig. 1. Experimental model of pontine hemorrhage in the rat. **A:** Schematic showing stereotaxic needle placement into the right ventral pontine tegmentum (**Insets:** coordinates [upper]; cranial aspect of bregma [*open arrowhead*] and the infusion site [*closed arrowhead*]; sagittal demonstration with the *dotted line* at craniocaudal level of infusion [lower]). **B:** Photograph of coronal section of tissue at 24 hours after collagenase (0.15 U) infusion, showing the hematoma surrounded by vasogenic edema (outlined with *dotted lines*). Bar = 1 mm. **C:** Representative H & E-stained cryosection (12 hours, 0.3 U collagenase) illustrating the hemorrhage. Bar = 0.5 mm. (**Inset** showing the hematoma border [*asterisk*]. Bar = 20 μ m.) **D and E:** Gehan-Breslow survival analysis results at 24 hours and 30 days.

**Fig. 2.**

Hematoma consequences at 24 hours: hematoma volume assay (A), brain water (B), neuroscore (composite and Voetsch) (C), vascular permeability (D), and (E) semiquantification (left) of the collagen Type IV, ZO-1, and MMP-2 and -9 protein immunoblots (right). Values are expressed as the mean \pm SEM ($n = 10$ [neuroscore] and $n = 5$ [all others]). * $p < 0.05$ compared with controls (sham and needle trauma). † $p < 0.05$ compared with collagenase infusion (0.15 U). Circles in bars indicate the raw data points of each measurement, and whiskers represent the SEM. OD = optical density.

**Fig. 3.**

Neurofunctional profiles in 30-day period: Voetsch score (**A**), locomotion (**B**), body weight (**C**), wire suspension (**D**), beam balance (**E**), and inclined plane (**F**). Values are expressed as mean \pm SEM ($n = 8$ [sham and needle trauma] and $n = 7$ [collagenase infusion, 0.15 units]). * $p < 0.05$ comparing collagenase infusion (*closed triangles*) with controls (sham, or needle trauma, *open circles*). path = path length.

**Fig. 4.**

Neurocognitive ability at 3 weeks. **A:** Motor learning assessed by the change in the latency to falling off an accelerating rotarod (2 rpm/5 sec) preoperatively and across 4 daily blocks. **B:** Working memory quantified by the number of spontaneous alternations in the T-maze. **C:** Spatial learning assessed by the swim distance needed to find the visible (cued) versus the hidden (spatial) platforms in the water maze. **D:** Spatial memory was determined by the percent duration in the probe quadrant when the platform was removed. Values expressed as the mean \pm SEM (rotarod, cued and spatial water maze) and mean \pm 95% CI (T-maze and probe quadrant), $n = 8$ (sham and needle trauma), $n = 7$ (collagenase infusion, 0.15 U). * $p < 0.05$ compared with controls (sham and needle trauma). † $p < 0.05$ compared with preoperative (rotarod) or cued trials (spatial water maze). ‡ $p < 0.05$ compared with Block 1 (rotarod and spatial water maze).

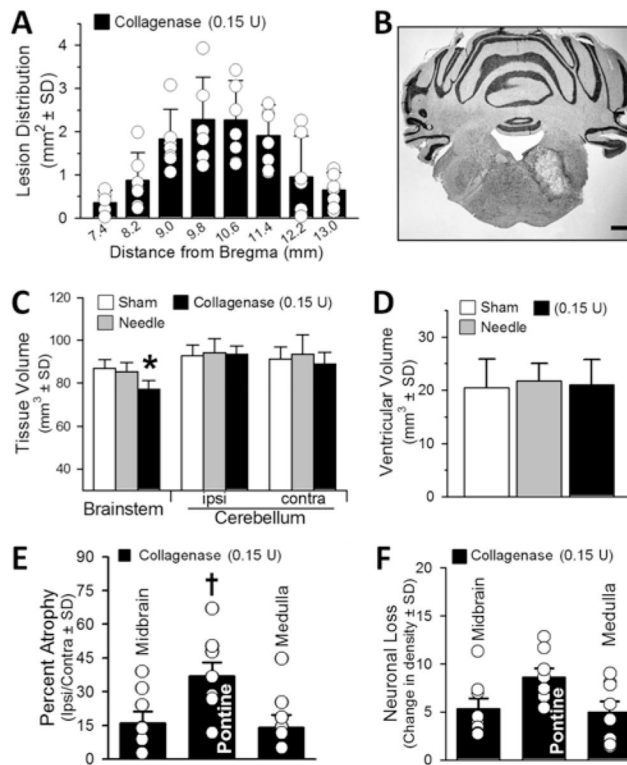


Fig. 5. Histopathological results at 30 days. **A:** Lesion distribution (in mm^2) throughout the brainstem. **B:** Representative cryosection illustrating the cystic cavity lesion. Bar = 1 mm. **C:** Infratentorial brain tissue volume (in mm^3). **D:** Volume of the ventricles (in mm^3). **E:** Percentage of atrophy of the brainstem (midbrain, pontine, and medulla), expressed as the volumetric difference between ipsilateral and contralateral sides. **F:** Neuronal density loss over the intact (perilesional) brainstem regions expressed as average difference in cell counts between ipsilateral and contralateral sides. Values expressed as the mean \pm SD ($n = 8$ [sham and needle trauma] and $n = 7$ [collagenase infusion, 0.15 U]). * $p < 0.05$ compared with controls (sham and needle). † $p < 0.05$ compared with midbrain and medulla (percentage of atrophy).

TABLE 1
Summary of physiological variables during and after collagenase infusion*

Group	Arterial Blood Gas				HR (per min)
	pH	PO ₂ (mm Hg)	PCO ₂ (mm Hg)	BP (mm Hg)	
during Tx					
sham	7.33 ± 0.03	186 ± 15	45 ± 3	81 ± 6	348 ± 40
needle	7.39 ± 0.02	184 ± 21	43 ± 5	89 ± 6	369 ± 28
CI-15 U	7.34 ± 0.05	192 ± 11	44 ± 8	89 ± 8	355 ± 33
CI-0.3 U	7.32 ± 0.03	187 ± 5	46 ± 5	91 ± 5	362 ± 25
30 mins after Tx					
sham	7.32 ± 0.01	185 ± 20	48 ± 5	84 ± 6	347 ± 48
needle	7.38 ± 0.05	186 ± 14	44 ± 3	88 ± 8	359 ± 14
CI-0.15 U	7.30 ± 0.08	188 ± 10	48 ± 9	88 ± 10	351 ± 33
CI-0.3 U	7.29 ± 0.03	173 ± 17	50 ± 9	90 ± 5	380 ± 37
24 hrs after Tx					
sham	7.50 ± 0.04	192 ± 12	36 ± 5	84 ± 5	348 ± 20
needle	7.52 ± 0.02	181 ± 7	37 ± 7	78 ± 3	361 ± 17
CI-0.15 U	7.47 ± 0.03	188 ± 11	38 ± 4	85 ± 9	359 ± 34
CI-0.3 U	7.38 ± 0.06	179 ± 14	49 ± 9	90 ± 9	329 ± 46
30 days after Tx					
sham	7.5 ± 0.06	182 ± 28	37 ± 8	94 ± 4	369 ± 9
needle	7.47 ± 0.03	192 ± 12	36 ± 4	83 ± 5	364 ± 27
CI-0.15 U	7.47 ± 0.03	190 ± 44	35 ± 4	87 ± 2	358 ± 39

* There was no statistically significant difference between groups. Values are presented as the mean ± SD. Abbreviations: BP = blood pressure; CI = collagen infusion; HR = heart rate; Tx = treatment.

TABLE 2
Summary of the modified Voetsch neuroscores

Test	Score			
	3	2	1	0
head movement (spontaneous)	moves in all dimensions	prefers 1 side	only to 1 side	flexed to 1 side
lethargy (confrontation)	fully responsive	moderately responsive	minimally responsive	coma
hearing (auditory startle)	finger rub	snap of fingers	loud clap	no startle
pain reflex (ear pinch)	brisk & symmetrical reaction	slightly diminished or asymmetrical reaction	greatly diminished & asymmetrical reaction	no reaction
corneal reflex (sensorimotor)				
proprioception (vibrissae)				
sensation (neck)				
exploration (5 mins in cage)	reaches 2 walls	reaches 1 wall	moves along base	no movement
circling (craniocaudal)	bilat turns	prefers 1 side	only to 1 side	falls to 1 side
sensation (axial)	brisk & symmetrical reaction	slightly diminished or asymmetrical reaction	greatly diminished & asymmetrical reaction	no reaction
4-limb movement (outstretch)	equal bilat	slight asymmetry	great asymmetry	paresis
forelimb movement (outstretch)				
climbing (motor function)	climbs to top	impaired climbing	stationary grip	falls immediately
beam (motor function)	explores both ends	some movement		